

Exploring Spectral Analysis: PSET 5

Benjamin Getraer

GEO 422: Data, Models, & Uncertainty in the Natural Sciences

January 16, 2018

Abstract

This is the paper's abstract . . .

1 Introduction

Introduction

Outline The remainder of this article is organized as follows. Section 2 introduces the implications of sampling and aliasing. Our new and exciting results are described in Section 4. Finally, Section 5 gives the conclusions.

2 Sampling and Recovery of Synthetic Signals

Nyquist sampling follows the theorem that for a given signal $f(x)$ composed of frequencies $\underline{\omega}$, $f(x)$ can be recovered using a sampling rate of $\frac{1}{\Delta x} \geq 2 \times \omega_{\max}$.

3 Recovery of Unknown Signals

The recovery of unknown signals from measurements can be approached in a similar fashion, with the sampling rate significantly affecting the frequencies detected in the signal. For instance, Figure 2 shows a time-series measured annually, while Figure 3 shows a time-series of the same phenomena measured every 10 years. The general process of analysis for each time-series went as follows:

1. The data \underline{d} were centered about their mean μ , and normalized by their variance σ^2 such that the normalized data $\underline{d}' = (\underline{d} - \mu) / \sqrt{\sigma^2}$.
2. The power-spectral-density of the \underline{d}' signal frequencies $\underline{\omega}$ were estimated by Fourier transform.
3. Periodic structures in the signal were estimated by the element-wise inversion of period $L = \omega^{-1}$.

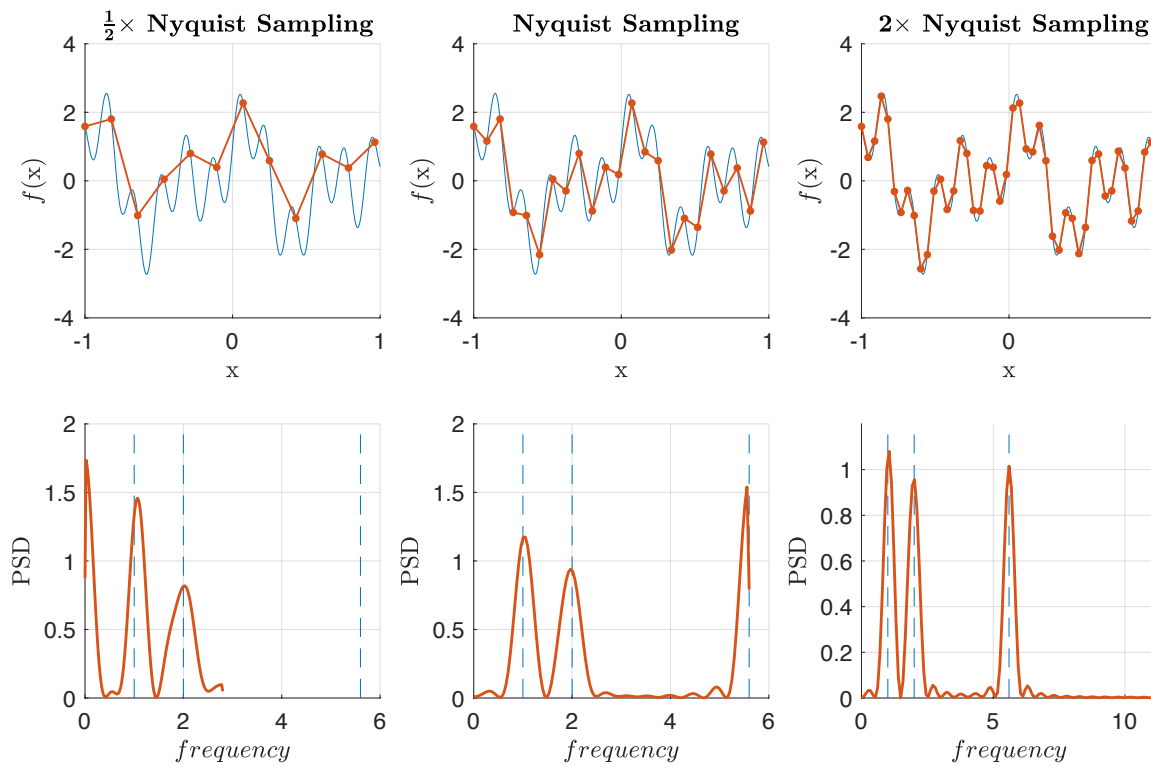


Figure 1: Sampling (in red) of the signal $f(x) = \cos(2\pi \times x) + \sin(2\pi \times 2x) + \sin(2\pi \times 5.6x)$ (in blue) at various sampling rates, where “Nyquist Sampling” is defined as a sampling rate of $\frac{1}{\Delta x} = 2 \times 5.6$.

4 Results

In this section we describe the results.

5 Conclusions

We worked hard, and achieved very little.

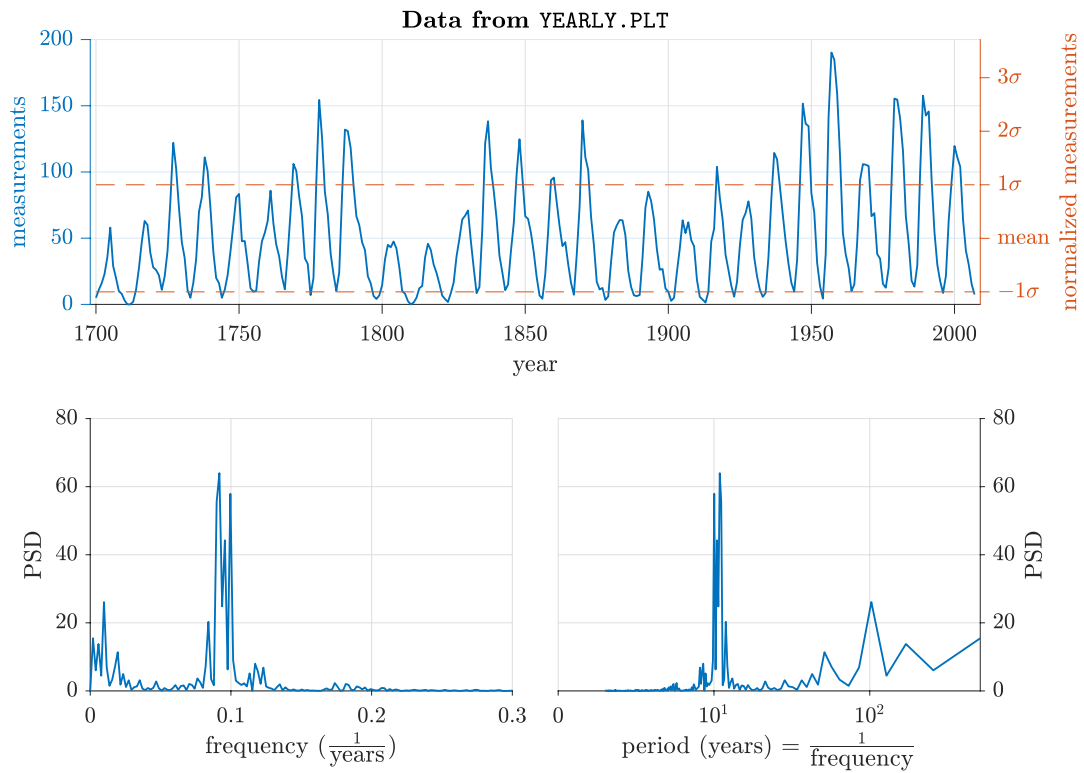


Figure 2: Analysis of time-series given in `YEARLY.PLT`. On top are the data \underline{d} with a normalized axis on the right showing the dimensions of \underline{d}' (see Section 3). On bottom left is the power-spectral-density (PSD) of the \underline{d}' signal frequencies estimated by `PERIODOGRAM`, using the default box-car window. Inversion of the frequency shows periodic structure within the data around the 10 and 100 year time-scales (bottom right).

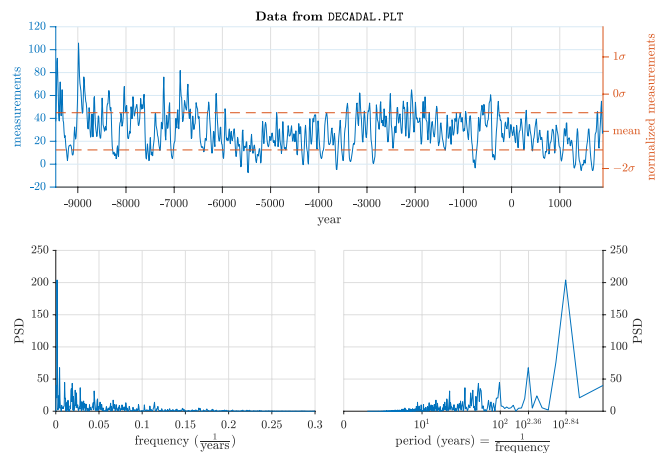


Figure 3: Analysis of time-series given in `DECADAL.PLT`. On top are the data \underline{d} with a normalized axis on the right showing the dimensions of \underline{d}' (see Section 3). On bottom left is the power-spectral-density (PSD) of the \underline{d}' signal frequencies estimated by `PERIODOGRAM`, using the default box-car window. Inversion of the frequency shows periodic structure within the data around the 10 and 100 year time-scales (bottom right).

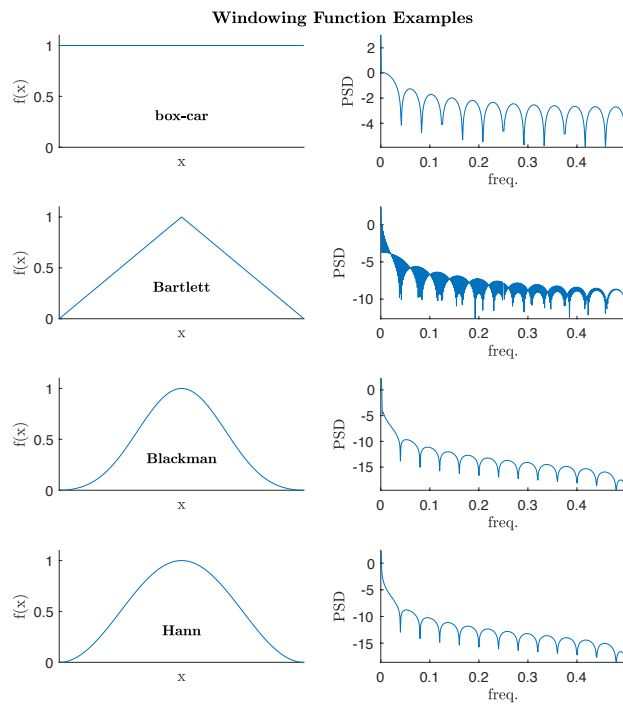


Figure 4: Examples of various windowing functions, over the domain $[-1, 1]$, of length 1000.

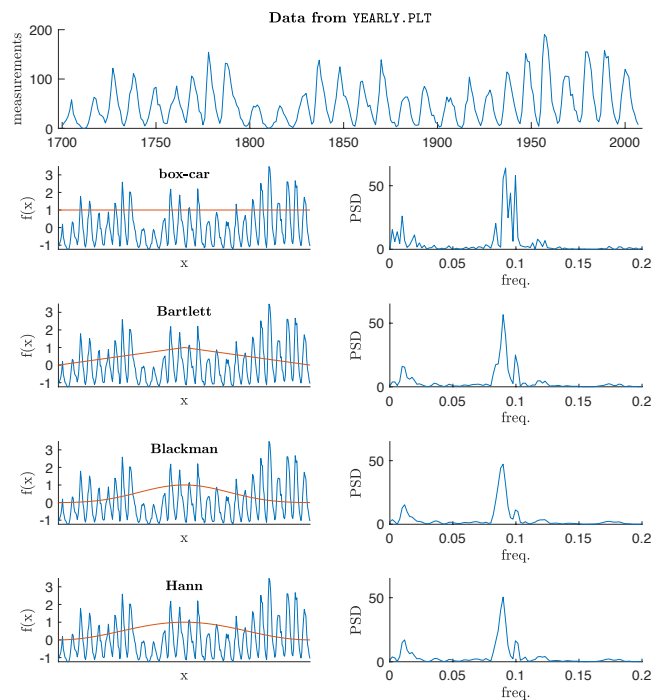


Figure 5: Demonstration of various windowing functions, using PERIODOGRAM and the YEARLY.PLT dataset. Note that the shape of the estimated PSD is different for each window function, but that all show peaks at frequencies $\omega = 0.1, 0.09, 0.0117$ corresponding to periods of $L = 10, 11.1, 85.5$ years.